Published in final edited form as:
J Mol Cell Cardiol. 2007 December ; 43(6): 792–801. doi:10.1016/j.yjmcc.2007.08.011.

Proteomic Alterations in Heat Shock Protein 27 and Identification of Phosphoproteins in Ascending Aortic Aneurysm Associated with Bicuspid and Tricuspid Aortic Valve

Peter Matt, MD[1], **Zongming Fu, PhD**[1], **Thierry Carrel, MD**[2], **David L. Huso, DVM, PhD**[3], **Stefan Dirnhofer, MD**[4], **Ivan Lefkovits, PhD**[2], **Hans-Reinhard Zerkowski, MD**[2,*], and **Jennifer Van Eyk, PhD**[1,*]

[1]Johns Hopkins Proteomics Center, Baltimore, USA [2]Division of Cardiac Surgery, University Hospital, Basel, Switzerland [3]Department of Molecular and Comparative Pathobiology, Johns Hopkins University, Baltimore, USA [4]Institute of Pathology, University Hospital, Basel, Switzerland

Abstract

Whether or not there are molecular differences, at the intra- and extracellular level, between aortic dilatation in patients with bicuspid (BAV) and those with a tricuspid aortic valve (TAV) has remained controversial for years. We have performed 2-dimensional gelelectrophoresis and mass spectrometry coupled with dephosphorylation and phosphostaining experiments to reveal and define protein alterations and the high abundant structural phosphoproteins in BAV compared to TAV aortic aneurysm samples. 2-D gel patterns showed a high correlation in protein expression between BAV and TAV specimens (n=10). Few proteins showed significant differences, among those a phosphorylated form of heat shock protein (HSP) 27 with significantly lower expression in BAV compared to TAV aortic samples (p=0.02). The phosphoprotein tracing revealed four different phosphoproteins including Rho GDP dissociation inhibitor 1, calponin 3, myosin regulatory light chain 2 and four differentially phosphorylated forms of HSP27. Levels of total HSP27 and dually phosphorylated HSP27 (S78/S82) were investigated in an extended patient cohort (n=15) using ELISA. Total HSP27 was significantly lower in BAV compared to TAV patients (p=0.03), with no correlation in levels of phospho-HSP27 (S78/S82) (p=0.4). Western blots analysis showed a trend towards lower levels of phospho-HSP27 (S78) in BAV patients (p=0.07). Immunohistochemical analysis revealed that differences in HSP27 occur in the cytoplasma of VSMC's and not extracellularly. Alterations in HSP27 may give early evidence for intracellular differences in aortic aneurysm of patients with BAV and TAV. Whether HSP27 and

Corresponding author: Peter Matt, MD, Johns Hopkins Proteomics Center, 5200 Eastern Avenue, 601 MFL Bldg. Center Tower, Baltimore, Maryland 21224, USA, Tel. 001 410 733 65 77, Fax. 001 550 85 12, pmatt1@jhmi.edu.
*These authors contributed equally to this work.

Disclosures
No disclosures.

the defined phosphoproteins have a specific role in BAV associated aortic dilatation remains to be elucidated.

Keywords

Proteomics; Heat shock protein 27; Phosphoprotein; Aortic aneurysm; Bicuspid aortic valve

Introduction

The bicuspid aortic valve (BAV) is a common congenital malformation with a prevalence of 1-2 % [1, 2]. It is often associated with acquired lesions of the ascending aorta, in particular aortic aneurysm. Different flow dynamics through the BAV and tricuspid aortic valve (TAV) may be one explanation for dilatative processes in the aorta. Whether or not there are molecular differences, at the intra- and extracellular level, between the aortic dilatation in patients with a BAV and those with TAV has remained controversial for years [3]. Most studies have focused on extracellular matrix alterations and have shown reduced and thinned elastic lamellae, differences in matrix metalloproteinases (MMP-2, MMP-9), tissue inhibitor metalloproteinases (TIMP-1, TIMP-2) and reduced levels of fibrillin-1 in BAV compared with TAV aortas [4-7]. Furthermore, there is an increased proportion of vascular smooth muscle cell (VSMC) apoptosis in BAV aortas compared with TAV samples [6]. Recent transmission electron microscopy (TEM) investigations found, in BAV aortas, a large number of structurally abnormal VSMCs and a loss of close attachment of VSMCs to their surrounding elastic lamellae [8]. This suggests that VSMC alterations may be a key to understanding aortic aneurysm formation. In this respect, post-translational modifications of proteins, including phosphorylation could represent an important regulatory event in VSMC cell shape, contraction and migration are regulated, at least in part, by phosphorylation of high abundant cytoskeletal and myofilament proteins. As such, the identification of high abundant structural proteins and the assessment of their phosphorylation status in aortic lesions obtained from BAV and TAV patients is expected to provide insight into the dominant difference. The aim of this study is to compare two-dimensional gel electrophoresis (2DE) pattern of ascending aortic aneurysm specimen from patients with a BAV and TAV, and to reveal and define phosphoproteins in these samples. Validation was undertaken for one such protein, heat shock protein (HSP27), using ELISA, Western blot and Immunohistochemical based methods.

Our studies could demonstrate that 2DE pattern of ascending aortic aneurysm show a high degree of correlation between BAV and TAV patients. Among proteome alterations, HSP27 showed most consistent changes between both patient groups. Levels of total HSP27 were significantly lower in aortic samples from patients with a BAV which may be due, at least in part, to reduction of phosphorylated HSP27 (S78). Immunohistochemical analysis revealed that these differences occur mainly in the cytoplasma of VSMC`s and not extracellularly. In addition, we revealed and defined four different phosphoproteins using 2DE and mass spectrometry, all four phosphoproteins have functional implementations in the actin-based cytoskeleton.

Materials and Methods

Tissue Handling, Protein Extraction

Aortic wall segments were excised from 16 patients undergoing aortic aneurysm surgery from the anterior part of the ascending aorta 3 to 4 cm above the aortic annulus. Informed consent was obtained from all patients before enrollment. Aortic specimen were immediately placed in physiological solution (Krebs-Henseleit) to remove blood components, frozen in liquid nitrogen, and stored at -80°C until they were analyzed. Histology was carried out on all samples to exclude patients with arteriosclerosis.

All steps in the protein extraction protocol were carried out at 4°C. Samples were homogenized in extraction buffer consisting of (in mmol/L) HEPES 25 (pH 7.4), sodium fluoride 50, sodiumorthovanidate 0.25, phenylmethylsulfonyl fluoride 0.25, EDTA 0.5, leupeptin 1.25, pepstatin A 1.25 and aprotinin A 1.25. Samples were centrifuged at 14000 *g* for 5 min at 4°C, and the supernatant was saved as protein extract. Protein concentrations were obtained using BCA assay done in triplicate.

2-D Gel Electrophoresis

IEF was carried out using a Protean IEF cell (BioRad, Hercules, CA) according to the manufacturer's protocol. For the first dimension of separation 100ug of total protein was applied. Immobilized pH gradient (IPG) Dry Strip (gradient pH 3–10, 18 cm, GE Healthcare, Piscataway, CA) were actively rehydrated at 50 V for 10 h to enhance protein uptake, then subjected to the following conditions using a rapid voltage-ramping method: 100 V for 25 Vh, 500 V for 125 Vh, 1000 V for 250 Vh, and 8000 V for 85 kVh. For SDS-PAGE, IPG strips were incubated for 10 min in equilibration buffer (50 mmol/L Tris-HCl [pH 8.8], 6 mol/L urea, 30% vol/vol glycerol, 2% wt/vol SDS) supplemented with 10 mg/mL DTT, followed by a 10-min incubation in equilibration buffer supplemented with 25 mg/mL iodoacetamide, then rinsed once with SDS-PAGE buffer (25 mmol/L Tris, 192 mmol/L glycine [pH 8.3], 0.1% wt/vol SDS). IEF strips were then embedded in a 4% acrylamide stacking gel, and the proteins were resolved by SDS-PAGE using a Protean II XL system (BioRad, Hercules, CA). Electrophoresis was carried out at 50 V for 30 min, followed by 150 V for 7.5 h. In addition, a part of the 2DE was done in the Anderson's ISODALT system for the simultaneous analysis of 20 samples (instruments produced in the workshop of the former Basel Institute for Immunology, Switzerland) [9]. The first dimension of separation was a pH gradient nonlinear 3-10 and the second dimension 11-19% SDS-PAGE (Figure 1). Silver staining of the 2-D gel was performed according to the protocol of Shevchenko, which is compatible with subsequent protein analysis by mass spectrometry [10]. Image analysis was carried out using PDQuest (BioRad, Hercules, CA).

Assessment of phosphorylation status: Dephosphorylation and Phosphostaining

The aortic sample of a patient with a TAV was dephosphorylated with alkaline phosphatase using the following protocol: an aliquot of the aortic protein extract was divided into two equal volumes (100 μg each). Alkaline phosphatase reaction buffer (10x NE Buffer 3, New England Biolabs, Ipswich, MA) was added to each sample, 2 μL (10'000 U/ml) of calf intestinal alkaline phosphatase (New England Biolabs, Ipswich, MA) was added to one

sample, and then deionized distilled water was added to both samples to total volumes of 25 μl. Samples were mixed well and incubated at 37°C for 18 h. The reaction was stopped with isoelectric focusing (IEF) buffer, and samples were frozen at -80°C until further analysis.

The dephosphorylated and untreated samples were separated by 2DE as above except the 2DE gel underwent a phosphostaining procedure using Pro-Q Diamond phosphoprotein gel stain (Molecular Probes, Invitrogen, Carlsbad, CA) according to the manufacturer's protocol. Fluorescent staining of the SDS-polyacrylamide gels was performed by fixing the gels in 50% methanol–10% acetic acid overnight, washing with three changes of deionized distilled water for 10 min per wash, followed by incubation in Pro-Q Diamond phosphoprotein gel stain for 90 min, and destaining with three successive washes of 20% acetonitrile in 50 mM sodium acetate, pH 4 for 30 min each, and two final washes with deionized distilled water.

Each protein sample, with and without dephosphorylation or with phosphostaining, was labeled with 400 pmol of Cy3 or Cy5 *per* 50 ug protein according to the manufacturer's protocol (GE Healthcare, Piscataway, NJ). As the internal control for 2-D DIGE, a mixed protein sample mixture that contained equal amounts of each sample (dephosphorylated and non-dephosphorylated) for analysis was labeled with Cy2. After labeling, 50 ug of Cy2-, Cy3-, and Cy5-labeled protein samples were separated in the same 2-D gel. Gels were then restained with silver as described previously, in order to allow visualization of spots needed for spot picking and subsequent MS analysis. Images for all Cy dye stained gels were collected using the Typhoon 9410 (GE Healthcare, Piscataway, NJ) fluorescence gel scanner. The Cy2-labeled gel images were collected using a 488 nm laser as excitation source and an emission filter of 520 nm BP (band pass) 40. The Cy3-labeled gel images were collected using a 532 nm laser as excitation source and an emission filter of 580 nm BP30. The Cy5-labeled gel images were collected using a 633 nm laser as excitation source and an emission filter of 670 nm BP30.

Protein Identification by Mass Spectrometry, Bioinformatic Data Analysis

Protein spots extracted from silver-stained 2DE gels were destained according to Gharahdaghi, then dried under vacuum before enzymatic digestion with sequence-grade modified trypsin (Promega, Madison, WI) [11]. Samples were analyzed using a Voyager DE-STR matrix-assisted laser desorption/ionization time-of-flight (MALDI-TOF) mass spectrometer (Applied Biosystems, Foster City, CA). The data from the spectra were used to identify proteins by peptide mass fingerprinting, using the MASCOT program and comparing with NCBI protein sequence databases.

2-D Western Blot HSP27

1-D gels were performed as described above using immobilized pH gradient (IPG) Dry Strip (gradient pH 3–10, 18 cm, GE Healthcare, Piscataway, NJ). IEF strips were cut between pH 3.5-6.5 and resolved for the 2nd dimension by NuPAGE® Novex 4-12% Bis-Tris Mini-gels (Invitrogen, Carlsbad, CA) using the XCell *SureLock*™ Mini-Cell system (Invitrogen, Carlsbad, CA). From 2-D gels, proteins were transferred to nitrocellulose membranes using a wet transfer cell. The blots were blocked with 5% non-fat dry milk in TBST overnight at

4° C with gentle agitation. The blots were probed with a primary mouse monoclonal antibody to HSP27 (Abcam, Cambridge, MA) for 1 h at 4° C, washed three times with TBST and incubated with appropriate horseradish peroxidase-labeled secondary antibodies for 1 h at 4° C. The immunopositive bands were visualized by enhanced chemiluminescence (Immun-Star AP, BioRad, Hercules, CA).

Enzyme-Linked Immunosorbent Assay (ELISA)

Aortic levels of total HSP27 and specific HSP27 (dually phosphorylated at serine 78 and 82) were measured in sixteen aortic samples. Aortic extracts, as used for 2DE, were analyzed using the DuoSet IC ELISA kit (R&D Systems, Minneapolis, MN, catalog No. DYC 1580-2, DYC 2314-2) according to the manufacturer's protocol. ELISA wells were precoated with goat anti-human HSP27/anti-human phospho-HSP27 monoclonal antibody overnight at room temperature. The plates were washed, blocked and the samples and standards added. After incubation for two hours and washing, a biotinylated rabbit anti-human HSP27/anti-human phospho-HSP27 detection antibody was added. After another washing, samples were incubated with Streptavidin-horseradish-peroxidase for 20 minutes. After adding of substrate solution and the reaction had been stopped by addition of 2N sulfuric acid, the optical density of each well was measured immediately with a microplate reader at 450nm, the wavelength correction was set to 570nm.

Western Blot Analysis

Equal amounts (10ug) of eight aortic samples (four with a TAV and four with a BAV) were loaded on NuPAGE® Novex 4-12% Bis-Tris Mini-gels (Invitrogen, Carlsbad, CA) and resolved using the XCell *SureLock*™ Mini-Cell system (Invitrogen, Carlsbad, CA). Gels were transferred to nitrocellulose membranes using a wet transfer cell. The blots were blocked with 5% BSA in TBST overnight at 4° C, then probed with primary rabbit antibodies to phospho-HSP27 (S15, S78, S82) (Abcam, Cambridge, MA) for 1 h at 4° C. The blots were washed three times with TBST and incubated with appropriate horseradish peroxidase-labeled secondary antibodies for 1 h at 4° C. The immunopositive bands were visualized by enhanced chemiluminescence (Immun-Star AP, BioRad, Hercules, CA) and the resulting bands quantified by Progenesis software (Nonlinear USA Inc, Durham, NC).

Immunohistochemistry HSP27

For immunohistochemistry, tissues were obtained from aorta specimens that had been archived as unfixed, frozen specimens. The tissues were thawed and fixed in fresh 4% paraformaldehyde for 48 hours, processed and embedded in paraffin and sectioned at 5 microns. Sections were deparaffinized followed by heated citrate buffer antigen retrieval, protein and endogenous peroxide blocking, and stained using monoclonal antibody to HSP27 (Abcam, Cambridge, MA). Monoclonal antibody to an irrelevant viral protein was used on control sections. The slides were developed according to manufacturer's instructions in the LSAB2 kit (DAKO, Carpinteria, CA).

Statistical Analysis

For statistical analysis of patients' baseline characteristics, ELISA and Western blot data the Chi Square, Fisher`s exact, Mann-Whitney U and student`s t-tests were used as appropriate (with SPSS 8.0).

Results

2DE assessment of high abundant proteome changes

Patients baseline characteristics were not significantly different between the two groups (Table 1). Silver-stained 2-D gels (Figure 1 shows a representative pH 3-10 gel) of aortic samples obtained from ten male patients, five had a BAV and five a TAV, showed similar numbers of protein spots with median 564 (512-583) in BAV and 576 (532-584) in TAV samples (p=0.6). Analysis of 2-D gel patterns showed a high degree of correlation in protein expression among BAV and TAV samples, and quantitative comparison revealed only few protein spots with different expression between experimental groups. One spot (see arrows in Figure 1) was significantly lower expressed (=medium densitometric values) in BAV compared to TAV specimens (p=0.02). MALDI-TOF mass spectrometry identified the spot as heat shock protein 27.

2DE assessment of the phosphoproteome

The aortic sample was dephosphorylated using alkaline phosphatase and analyzed by 2DE with validation using a complementary phosphostain. The experiment was designed to capture three (or in some instances two) Cy-dye-labeled images derived from a single gel scanning of the same sample. Figure 2 (representative gel images) shows the endogenous phosphorylated proteins (red) which were dephosphorylated upon treatment with phosphatase (green). Specifically, five phosphorylated (spots 1 to 4, and 7) and eight dephosphorylated (spots 5, 6, 8 to 13) protein spots were observed and confirmed using a phospho-specific protein stain (numbers on Figure 2). The phospho-stain confirmed four phosphoproteins (spots 1, 2, 3 and 7). Figure 3 shows a magnified corresponding area of the 2-D DIGE experiments and the corresponding silver-stained 2-D gels without and with dephosphorylation. Analysis and comparison of these phosphoproteins in silver-stained 2-D gels revealed a statistical significant difference between both experimental groups only in spot number 2. However, spot 4, 6, 8, 10, 12 and 13 were of low abundance in all silver-stained 2-D gels, which makes an appropriate statistical analysis (of densitometric values) difficult. To identify phosphoproteins and dephosphorylated proteins, spots were excised from corresponding silver-stained 2-D gels, digested and analyzed using a MALDI-TOF mass spectrometer for protein identification (see Table 2 for protein identification, protein accession number, mass, score and documented protein function). Heat shock protein 27 was once more identified in 4 protein spots, three of which were phosphorylated. In addition, we identified Rho GDP dissociation inhibitor (Rho GDI 1), calponin 3 and myosin regulatory light chain 2 (MLC20). Several other protein spots could not be identified, even when the same spot was combined from multiple gels, due to their low protein expression in the 2-D gel.

2D assessment of HSP27

Separation (of the same aortic sample used for phosphoproteome analysis) by 2-D Western blot revealed additional HSP27-antibody reactive spots other than the ones previously identified by 2DE and MS. Figure 4 illustrates these protein spots: number 2, 3 and 4 correspond to phosphorylated forms of HSP27 (as shown in the phosphoproteome experiments in Figure 2 and 3).

Quantification of total HSP27 and phospho-HSP27 (S78/S82) in an expanded patient cohort

Aortic samples of an expanded patient group were analyzed to HSP27 quantity. There were no statistical significant differences in patients' characteristics between the experimental groups (Table 1). Based on ELISA analyses of tissue homogenates, the quantity of total HSP27 in aortas obtained from the expanded study group (n=15, Figure 5) was increased by 1.4 fold in TAV patients compared to BAV patients: the mean of total HSP27 was 360.7 ng/ml (SD ± 86.6) in TAV patients and 264.5 ng/ml (SD ± 94.9) in samples from BAV patients (p=0.03). The mean of phosphorylated HSP27 (note only monitoring dually phosphorylated S78 and S82) did not differ (p=0.4) between experimental groups. Total HSP27 or phospho-HSP27 (S78/S82) levels showed no correlation to gender, age or type of aortic valve failure (stenosis or insufficiency).

Quantification of phospho-HSP27 (S15, S78, S82)

Figure 6. illustrates Western blots of phospho-HSP27 (S78) and phospho-HSP27 (S15). Phospho-HSP27 (S78) showed in some aortic samples two bands, one of those may correspond to the dually phosphorylated HSP27 (as analyzed by ELISA). Levels of the more intense band of phospho-HSP27 (S78) showed a trend towards lower concentrations in aortic samples from patients with a BAV (p=0.07). Western blot analysis of phospho-HSP27 (S15) showed low levels in both experimental groups with no significant difference. Western blots of phospho-HSP27 (S82) showed no band throughout aortic samples (data not shown).

HSP27 Immunostaining

Immunohistochemical analysis revealed that HSP27 is mainly expressed in the cytoplasma of VSMC`s (around their nuclei, Figure 7). Therefore, differences in total HSP27 and phospho-HSP27 (S78) between BAV and TAV patients likely reflect alterations inside VSMC`s and not extracellularly. Figure 7 illustrates differences in HSP27 immunostaining in aortic sections of a patient with TAV and BAV.

Discussion

Patients with a BAV are more likely to develop aortic complications during their lifetime than are patients with a TAV [1]. Hemodynamic flow and turbulences across the aortic valve differ in those with a BAV and those with a TAV and may be one reason for acquired aortic lesions. However, it is known that patients with a BAV develop aortic aneurysm even with a normally functioning aortic valve and years after aortic valve replacement [12]. It is still unclear what type of genetic deletion causes a BAV, NOTCH1 haplo-insufficiency may play a role in familial BAV [13]. Whether or not there is an intrinsic defect in the aortic wall of

BAV patients has remained controversial for years. Several studies have previously compared aortic aneurysm samples from patients with a BAV and a TAV, however, most of them focused on extracellular matrix alterations [4]. Several studies have focused on VSMC alterations, but these have shown changes in their phenotype which may contribute to the aneurysm formation [6]. Schmid compared BAV and TAV aneurysmatic samples and found that BAV aortas had an increased proportion of VSMC apoptosis [6]. Do and colleagues revealed, in a recent study using light microscopy and TEM, that BAV aortas had less elongated and more rounded VSMCs with an increased proportion of cytoplasmic degeneration and a loss of interdigitation of VSMCs with surrounding elastic lamellae [8]. VSMCs in the ascending aorta and aortic valve cusps are derived from the same neural crest such that common pathogenetic mechanisms leading to a BAV and aortic complications can be expected [13]. Alterations in VSMCs may be a key to understanding differences in aortic aneurysm formation between BAV and TAV patients [14].

Our hypothesis is that aortic aneurysm specimen from patients with a BAV and TAV have protein alterations that can be revealed by proteomics. Therefore, 2DE and MS analyzes were undertaken on dilated aortic samples from BAV and TAV patients undergoing aortic surgery. Furthermore, due to issues in collection, samples from “healthy control” were not included as part of the study design. This is supported by the high correlation in the 2DE of aortic specimen among BAV and TAV patients. Few protein spots were significantly different, among those the most consistent change was in HSP27 which was identified by MALDI-TOF mass spectrometry. This protein spot was significantly lower expressed in silver-stained 2-D gels of patients with a BAV compared with TAV ($p=0.02$). Other protein alterations occurred throughout the aortic specimens, however, those variations were inconsistent, appeared individually and did not correlate with the type of valve failure, aortic dimensions and patient age. It is known that HSP27 can be phosphorylated at least at four different serine sites (15, 78, 82 and 85) [15]. To evaluate whether the identified HSP27 spot is phosphorylated or not, 2DE coupled with dephosphorylation experiments and phosphostaining was performed and four forms of HSP27 were identified (3 phospho, 1 unphosphorylated). Overall, assessment of the phosphoproteome revealed that the form of HSP27, which is lower expressed in silver-stained 2-D gels of BAV aortas, must be phosphorylated (see number 2 in Figure 2 and 3). LC-MS/MS (liquid chromatography mass spectrometry), however, was not yet able to define these phosphorylation sites.

HSP27 is a chaperone protein preferentially expressed by VSMCs and endothelial cells. It can, if phosphorylated (=activated), bind, stabilize and rearrange intracellular actin microfilaments [16, 17]. HSP27 supports the formation of actin stress fibers and stabilizes the integrity of the cell. It maintains intracellular levels of reduced glutathione and leads to increased physical and chemical stress resistance. HSP27 is mainly phosphorylated by mitogen-activated protein kinase activated protein kinase 2 after cell stress [18]. We performed ELISA measurements of total HSP27 and phosphorylated HSP27 (dually phosphorylated at serine 78 and 82) in fifteen patients with aortic aneurysm, six patients had a BAV and nine patients had a TAV. Baseline characteristics did not significantly differ between the patient groups. ELISA results showed significantly higher levels of total HSP27 in TAV compared with BAV aortas ($p=0.03$, Figure 5). Phosphorylated HSP27 (S78/S82) did not differ significantly between aortic samples ($p=0.4$). Western blot analysis of

phosphorylated HSP27 (S78) revealed a trend towards lower levels in patients with BAV (p=0.07, Figure 6), phosphorylated HSP27 (S15) or phosphorylated HSP27 (S82) showed low protein levels in both experimental groups without significant differences. Immunohistochemical analysis showed that differences in HSP27 occured mainly in the cytoplasma of VSMC`s and not extracellularly (Figure 7). These results suggest that alterations in HSP27 levels may be based, at least in part, on differences in intracellular HSP27 phosphorylated at S78. However, there are several other protein forms of HSP27, as shown in 2-D Western blot analysis (Figure 4), and one can not exclude the possibility that other (currently unidentified) phosphorylated amino acid residues or post-translational modificated forms of HSP27 are changing.

Park and colleagues recently demonstrated that total HSP27 and phosphorylated HSP27 is decreased in arterial plaques compared to nearby normal-appearing lesions [19]. Interestingly, levels of phosphorylated HSP27 were very little in the diseased area. This led to the hypothesis that induction of phosphorylated HSP27 protects against arteriosclerosis [20], which itself may promote aortic aneurysm formation. However, a decrease in HSP27 may also reflect the presence of high levels of proteases known to degrade HSP27 [21]. Higher expression of certain MMPs in aortic tissue of patients with a BAV compared to TAV is well known [4-7]. Levkau and colleagues showed that down-regulation of HSP27 increases the rate of cell apoptosis and subsequently leads to higher levels of MMP 2 [22]. In contrast, up-regulation of HSP27 leads to an overexpression of MMP 9 [23]. Le Maire recently found such an increase in MMP 2 in BAV samples but also increased MMP 9 levels in TAV aortas [7]. These data match with our data of lower HSP27 levels in aortic samples from patients with a BAV as compared to TAV.

Demographic parameters such as age, arterial hypertension or smoking history may differ between patients with a BAV and TAV and could influence the expression of HSP27. This may be connected to different stages of arteriosclerosis among aortic samples which, as described above, could alter HSP27 levels. In addition, flow dynamics across the bicuspid and tricuspid aortic valve could lead to a different extent of physical and chemical stress on the aortic wall which could influence HSP27. Most intriguingly, differences in total and phosphorylated HSP27 expression could reflect protective mechanisms in VSMCs that may be less pronounced within BAV aortas.

The phosphorylation/dephosphorylation experiments indicated that other proteins were phosphorylated (5 phosphorylated and 8 dephosphorylated protein spots in the 2-D gel pattern were observed (Figure 2 and 3)). This included Rho GDP dissociation inhibitor 1 (Rho GDI 1), calponin 3 and myosin regulatory light chain 2 (MLC20). All three proteins have functional implementations in actin-based cytoskeletal and or contractile function of the VSMC as described below.

Rho GDI 1 is a cytoplasmic protein that is expressed in a variety of cells including VSMC. It regulates the GDP/GTP exchange reaction of Rho proteins by inhibiting the dissociation of GDP and thus controlling the Rho dependent kinase signaling cascade. Rho GDI 1 is involved in several aspects of the actin cytoskeleton organisation, but also regulates cell morphology, motility and SMC contraction. Leffers revealed that overexpression of Rho

GDI 1 leads to loss of cytoplasm stress fibers, degradation of the actin cytoskeleton and a decrease in focal contact sites among SMCs [24].

Calponin 3 belongs to a family of actin-binding proteins, and is expressed in the cytoplasm of VSMCs and non-VSMCs. Calponin isoforms are thought to be involved in several biological processes, for example the regulation of muscle contraction, organization of the actin cytoskeleton and cell signaling at the surface membrane of VSMCs [25]. Calponin 3 represents the acidic isoform of Calponin, and may be less involved in the contraction process but is more part of the actin cytoskeleton.

MLC20 is mainly expressed in SMC tissue. It is of importance in the cell contractile activity, but also in the organization of the actin cytoskeleton. The interaction between actin and myosin is regulated through the phosphorylation of MLC20 by the enzyme myosin light chain kinase. Fazal showed that dephosphorylation of MLC20 leads to a destabilization of the actin cytoskeleton and VSMC apoptosis [26].

Further studies are required to tease out the role of phosphorylation of the cytoskeletal/ contractile proteins and the identification of the novel sites in HSP27 on aortic aneurysm formation. In this context, it is interesting to know that patients with a non-receptor protein tyrosine phosphatase defect (*e.g. Noonan syndrome*) show large aortic aneurysms [27, 28]. Knowing that the four identified phosphoproteins are expressed in VSMCs and are important parts of, or at least are involved in, the regulation of the actin cytoskeleton may lend considerable biological significance to our findings. However, their specific role in ascending aortic aneurysm formation in BAV patients remains to be elucidated.

In conclusion, we could demonstrate that 2DE pattern of ascending aortic aneurysm show a high degree of correlation between BAV and TAV patients. Among proteome alterations, levels of total HSP27 were significantly lower in aortic samples from patients with a BAV compared to TAV, which may be due, at least in part, to a reduction of phosphorylated HSP27 (S78). Immunohistochemical analysis revealed that these differences occur inside the cytoplasma of VSMC`s and not extracellularly. In addition, we revealed and defined four different phosphoproteins using 2DE and MS. All four phosphoproteins have functional implementations in the actin-based cytoskeleton. Our results may give early evidence for intracellular differences in ascending aortic aneurysm formation between BAV and TAV patients. What leads to different HSP27 expression and whether the phosphoproteins are involved in molecular processes leading to aortic dilatation in BAV patients requires further investigation.

Acknowledgments

Peter Matt thanks Emmanuel Traunecker and Rodney Lui for technical support, Thomas Grussenmeyer for fruitful discussions concerning the proteomic pattern of aortic tissue and Franziska Bernet and Martin Grapow for patient data acquisition. Peter Matt is supported by the Swiss National Foundation, the Novartis Foundation and the Hippocrate Foundation Basel. Jennifer Van Eyk is supported by grants from the National Heart, Lung, and Blood Institute Proteomic Initiative (contract NO-HV-28120) and the Daniel P. Amos Family Foundation.

References

1. Ward C. Clinical significance of the bicuspid aortic valve. Heart. 2000; 83(1):81–5. [PubMed: 10618341]
2. Fedak PW, David TE, Borger M, Verma S, Butany J, Weisel RD. Bicuspid aortic valve disease: recent insights in pathophysiology and treatment. Expert Rev Cardiovasc Ther. 2005; 3(2):295–308. [PubMed: 15853603]
3. Fedak PW, Verma S, David TE, Leask RL, Weisel RD, Butany J. Clinical and pathophysiological implications of a bicuspid aortic valve. Circulation. 2002; 106(8):900–4. [PubMed: 12186790]
4. Bauer M, Pasic M, Meyer R, Goetze N, Bauer U, Siniawski H, et al. Morphometric analysis of aortic media in patients with bicuspid and tricuspid aortic valve. Ann Thorac Surg. 2002; 74(1):58–62. [PubMed: 12118804]
5. Fedak PW, de Sa MP, Verma S, Nili N, Kazemian P, Butany J, et al. Vascular matrix remodeling in patients with bicuspid aortic valve malformations: implications for aortic dilatation. J Thorac Cardiovasc Surg. 2003; 126(3):797–806. [PubMed: 14502156]
6. Schmid FX, Bielenberg K, Schneider A, Haussler A, Keyser A, Birnbaum D. Ascending aortic aneurysm associated with bicuspid and tricuspid aortic valve: involvement and clinical relevance of smooth muscle cell apoptosis and expression of cell death-initiating proteins. Eur J Cardiothorac Surg. 2003; 23(4):537–43. [PubMed: 12694773]
7. LeMaire SA, Wang X, Wilks JA, Carter SA, Wen S, Won T, et al. Matrix metalloproteinases in ascending aortic aneurysms: bicuspid versus trileaflet aortic valves. J Surg Res. 2005; 123(1):40–8. [PubMed: 15652949]
8. Do HL, Nataatmadja M, Stenzel D, Theodoropoulos C, W M. Abstract: Structural abnormalities in vascular smooth muscle cells in marfan syndrome and bicuspid aortic valve aneurysm. Circulation Supplement AHA. 2006
9. Anderson NG, Anderson NL. Analytical techniques for cell fractions. XXI. Two-dimensional analysis of serum and tissue proteins: multiple isoelectric focusing. Anal Biochem. 1978; 85:331–340. [PubMed: 646092]
10. Shevchenko A, Wilm M, Vorm O, M M. Mass spectrometric sequencing of proteins from silver-stained polyacrylamide gels. Anal Chem. 1996; 68:850–858. [PubMed: 8779443]
11. Gharahdaghi F, Weinberg CR, Meagher DA, Imai BS, M SM. Mass spectrometric identification of proteins from silver-stained polyacrylamide gel: a method for the removal of silver ions to enhance sensitivity. Electrophoresis. 1999; 20:601–605. [PubMed: 10217175]
12. Yasuda H, Nakatani S, Stugaard M, Tsujita-Kuroda Y, Bando K, Kobayashi J, et al. Failure to prevent progressive dilation of ascending aorta by aortic valve replacement in patients with bicuspid aortic valve: comparison with tricuspid aortic valve. Circulation. 2003; 108(Suppl 1):II291–4. [PubMed: 12970248]
13. Garg V, Muth AN, Ransom JF, Schluterman MK, Barnes R, King IN, et al. Mutations in NOTCH1 cause aortic valve disease. Nature. 2005; 437(7056):270–4. [PubMed: 16025100]
14. Nataatmadja M, West M, West J, Summers K, Walker P, Nagata M, et al. Abnormal extracellular matrix protein transport associated with increased apoptosis of vascular smooth muscle cells in marfan syndrome and bicuspid aortic valve thoracic aortic aneurysm. Circulation. 2003; 108(Suppl 1):II329–34. [PubMed: 12970255]
15. Beausoleil SA, Jedrychowski M, Schwartz D, Elias JE, Villen J, Li J, et al. Large-scale characterization of HeLa cell nuclear phosphoproteins. Proc Natl Acad Sci USA. 2004; 101(33): 12130–5. [PubMed: 15302935]
16. Loktionova SA, Kabakov AE. Protein phosphatase inhibitors and heat preconditioning prevent Hsp27 dephosphorylation, F-actin disruption and deterioration of morphology in ATP-depleted endothelial cells. FEBS Lett. 1998; 433(3):294–300. [PubMed: 9744814]
17. Gerthoffer WT, Gunst SJ. Invited review: focal adhesion and small heat shock proteins in the regulation of actin remodeling and contractility in smooth muscle. J Appl Physiol. 2001; 91(2): 963–72. [PubMed: 11457815]

18. Stokoe D, Engel K, Campbell DG, Cohen P, G M. Identification of MAPKAP kinase 2 as a major enzyme responsible for the phosphorylation of the small mammalian heat shock proteins. FEBS Lett. 1992; 313(3):307–13. [PubMed: 1332886]

19. Park HK, Park EC, Bae SW, Park MY, Kim SW, Yoo HS, et al. Expression of Heat Shock Protein 27 in Human Atherosclerotic Plaques and Increased Plasma Level of Heat Shock Protein 27 in Patients With Acute Coronary Syndrome. Circulation. 2006; 114:886–893. [PubMed: 16923754]

20. De Souza AI, Wait R, Mitchell AG, Banner NR, Dunn MJ, Rose ML. Heat Shock Protein 27 is associated with freedom from graft vassculopathy after human cardiac transplantation. Circ Res. 2005; 97:192–198. [PubMed: 15976317]

21. Wick G. The heat is on: heat-shock proteins and atherosclerosis. Circulation. 2006; 114:870–872. [PubMed: 16940202]

22. Levkau B, Kenagy RD, Karsan A, Weitkamp B, Clowes AW, Ross R, et al. Activation of metalloproteinases and their association with integrins: an auxiliary apoptotic pathway in human endothelial cells. Cell Death Differ. 2002; 9(12):1360–7. [PubMed: 12478473]

23. Hansen RK, Parra I, Hilsenbeck SG, Himelstein B, Fuqua SA. Hsp27-induced MMP-9 expression is influenced by the Src tyrosine protein kinase yes. Biochem Biophys Res Commun. 2001; 282(1):186–93. [PubMed: 11263990]

24. Leffers H, Nielsen MS, Andersen AH, Honore B, Madsen P, Vandekerckhove J, et al. Identification of two human rho gdp dissociation inhibitor proteins whose overexpression leads to disruption of the actin cytoskeleton. Exp Cell Res. 1993; 209:165–174. [PubMed: 8262133]

25. Burgstaller G, Kranewitter WJ, G M. The molecular basis for the autoregulation of calponin by isoform-specific C-terminal tail sequences. Journal of Cell Science. 2002; 115:2021–2029. [PubMed: 11973344]

26. Fazal F, Gu L, Ihnatovych I, Han Y, Hu W, Antic N, et al. Inhibiting myosin light chain kinase induces apoptosis in vitro and in vivo. Mol Cell Biol. 2005; 25:6259–66. [PubMed: 15988034]

27. Purnell R, Williams I, Von Oppell U, W A. Giant aneurysms of the sinuses of Valsalva and aortic regurgitation in a patient with Noonan's syndrome. Eur J Cardiothorac Surg. 2005; 28(2):346–8. [PubMed: 15964762]

28. Morgan JM, Coupe MO, Honey M, M GA. Aneurysms of the sinuses of Valsalva in Noonan's syndrome. Eur Heart J. 1989; 10(2):190–3. [PubMed: 2924789]

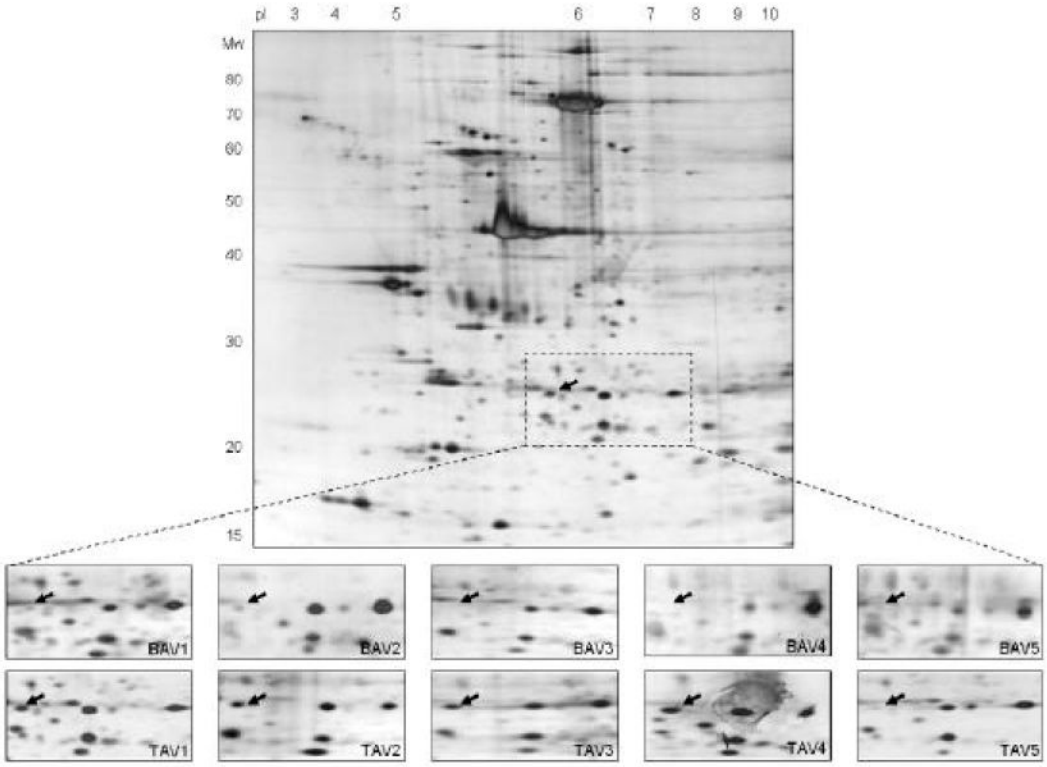

Figure 1.

Representative 2-D gel (pH gradient 3-10, 11-19% SDS-PAGE) of an aortic aneurysm sample from a patient with a TAV. Magnified 2-D pattern of five BAV (A1-A5) and five TAV (B1-B5) are shown. The arrows mark the spot that is significantly lower expressed (=medium densitometric values) in BAV compared to TAV specimen (p=0.02). The protein spot was identified as HSP27 using MALDI-TOF mass spectrometry, and corresponds to *number 2* in Figure 2 and 3.

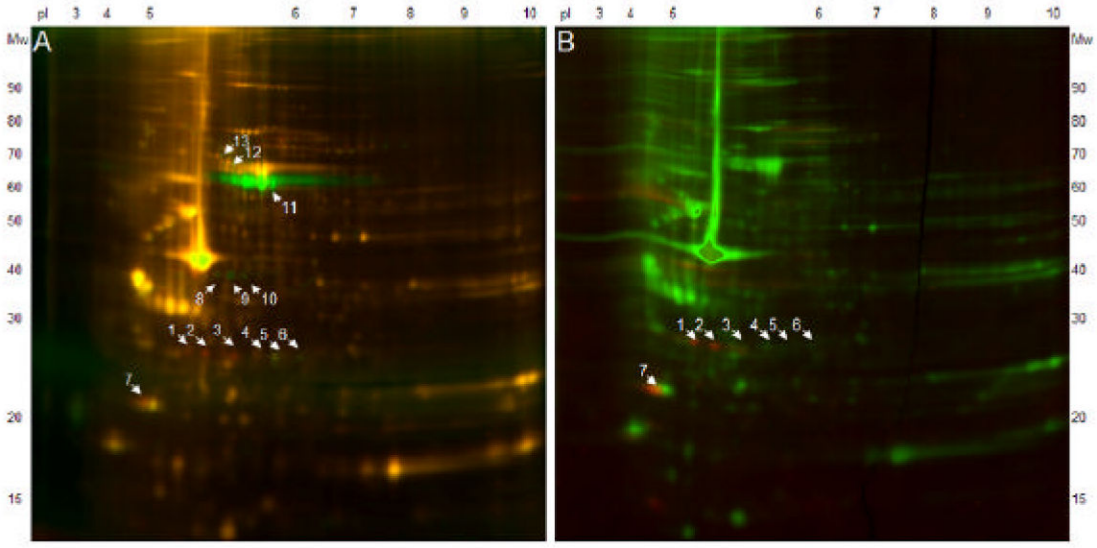

Figure 2.

2-D DIGE (pH gradient 3-10, 10% SDS-PAGE) after Dephosphorylation (A) and Phosphostaining (B). Red spots represent phosphoproteins, green spots in Figure A represent dephosphorylated proteins, yellow spots in Figure A and green spots in Figure B represent non-phosphorylated proteins. The dephosphorylation experiment revealed 5 phosphorylated (spot 1 to 4, and 7) and 8 dephosphorylated (spot 5, 6, 8 to 13) protein spots, phosphostaining revealed 4 phosphoproteins (spot 1 to 3, and 7).

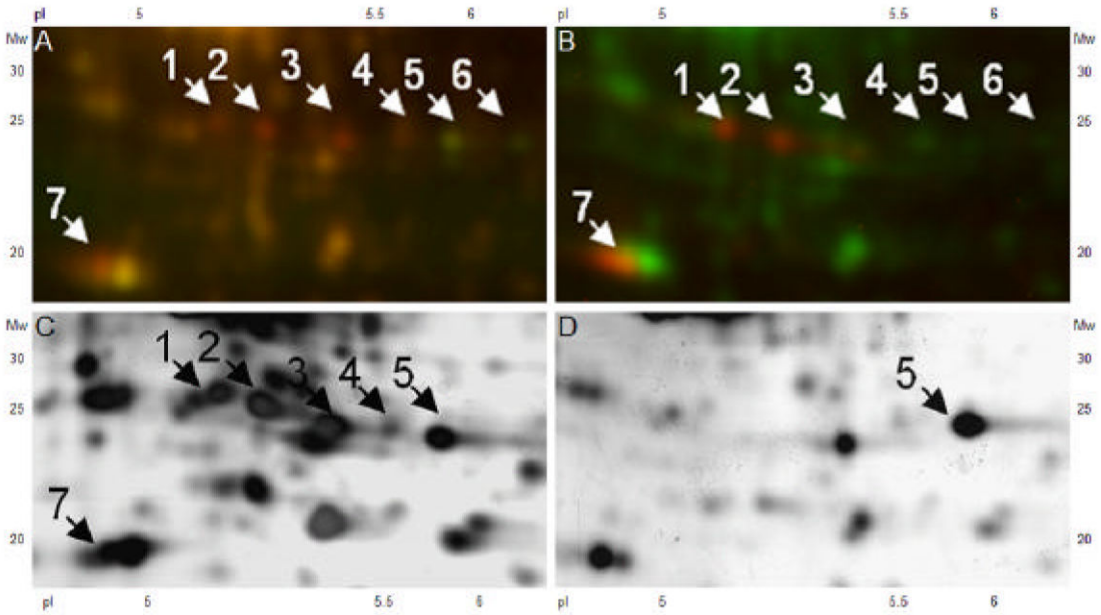

Figure 3.

Figure A and Figure B show enlarged areas of the 2-D DIGE experiments (shown in Figure 2, kDa 24-30, pI 5.2-6.4) without and with dephosphorylation. Red spots represent phosphoproteins, green spots in Figure A represent dephosphorylated proteins, yellow spots in Figure A and green spots in Figure B represent non-phosphorylated proteins. The same aortic sample is presented in a silver-stained 2-D gel without dephosphorylation in Figure C and with dephosphorylation in Figure D. Spots of interest were excized for MS identification.

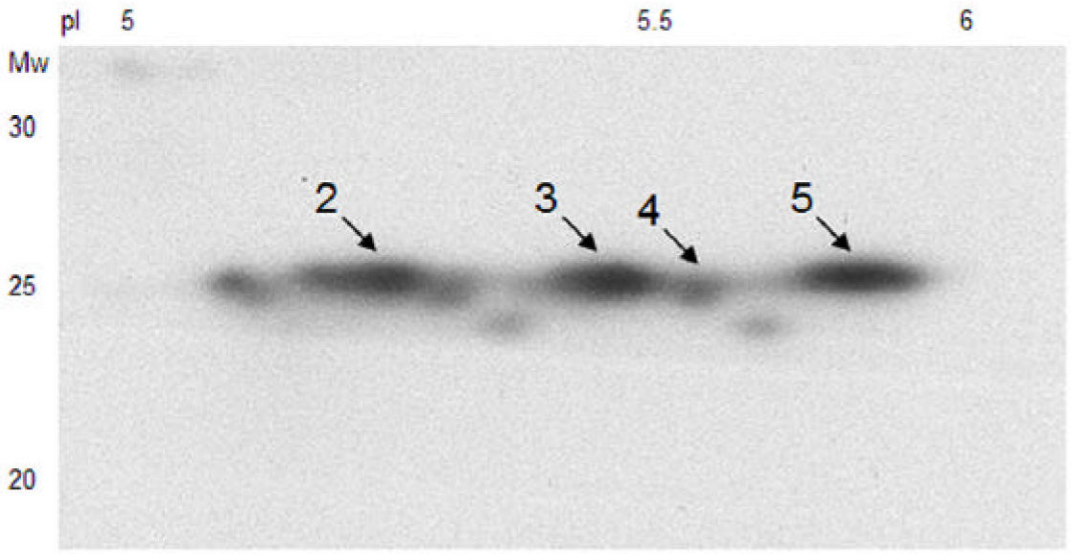

Figure 4.

2-D Western blot analysis of total HSP27 from the same sample used for Figure 2 and 3 (kDa 20-30, pI 5-6). Additional HSP27-reactive protein spots are shown compared to silver-stained 2-D gels and MS identification. Arrows and numbers mark corresponding spots to Figure 2 and 3.

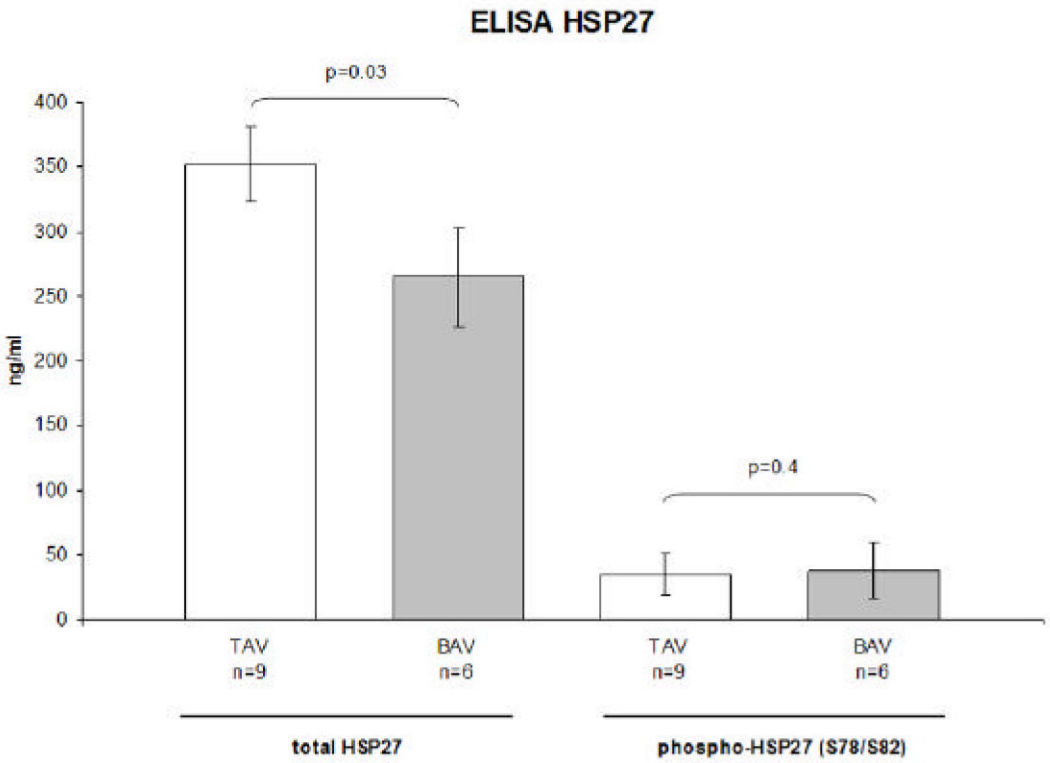

Figure 5.

Concentration of total HSP27 and phosphorylated HSP27 (S78/S82) in TAV (n=9) and BAV (n=6) aortic samples revealed from ELISA analysis. Data are in mean ± SEM. Quantity of total HSP27 shows a statistical significant difference between TAV and BAV aortas (p=0.03).

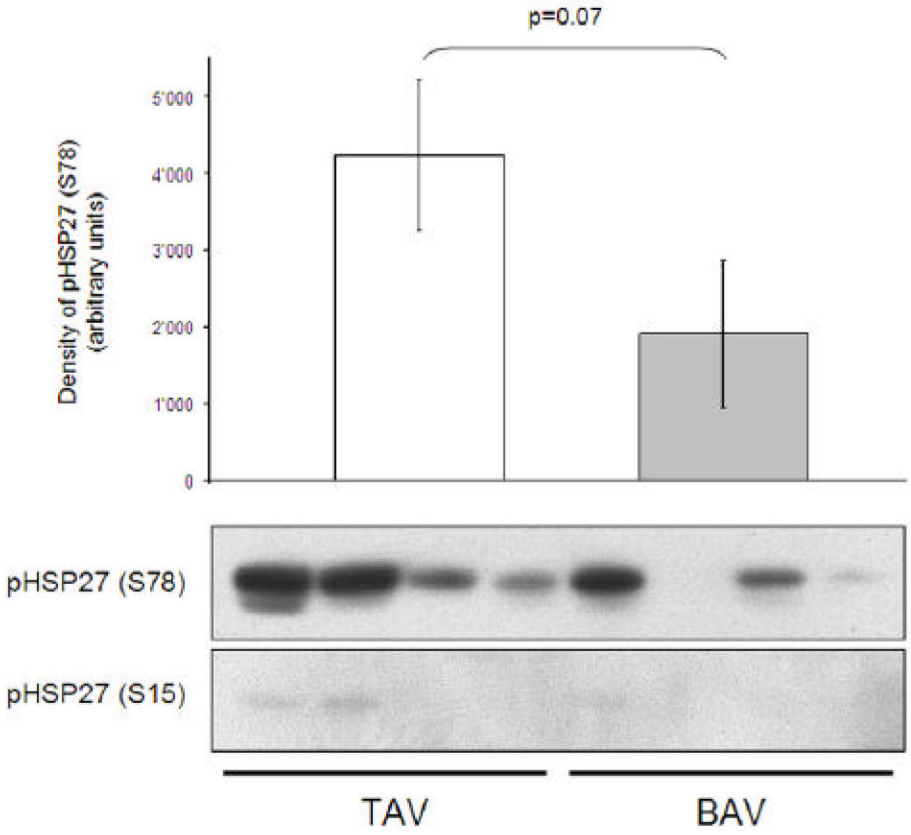

Figure 6.

Western blot analysis of phospho-HSP27 (S78) and phospho-HSP27 (S15) in aortic samples from patients with a TAV and BAV. Levels of phospho-HSP27 (S78) showed a trend towards a significant difference (p=0.07), levels of phospho-HSP27 (S15) were low in aortic samples of both experimental groups with no significant difference.

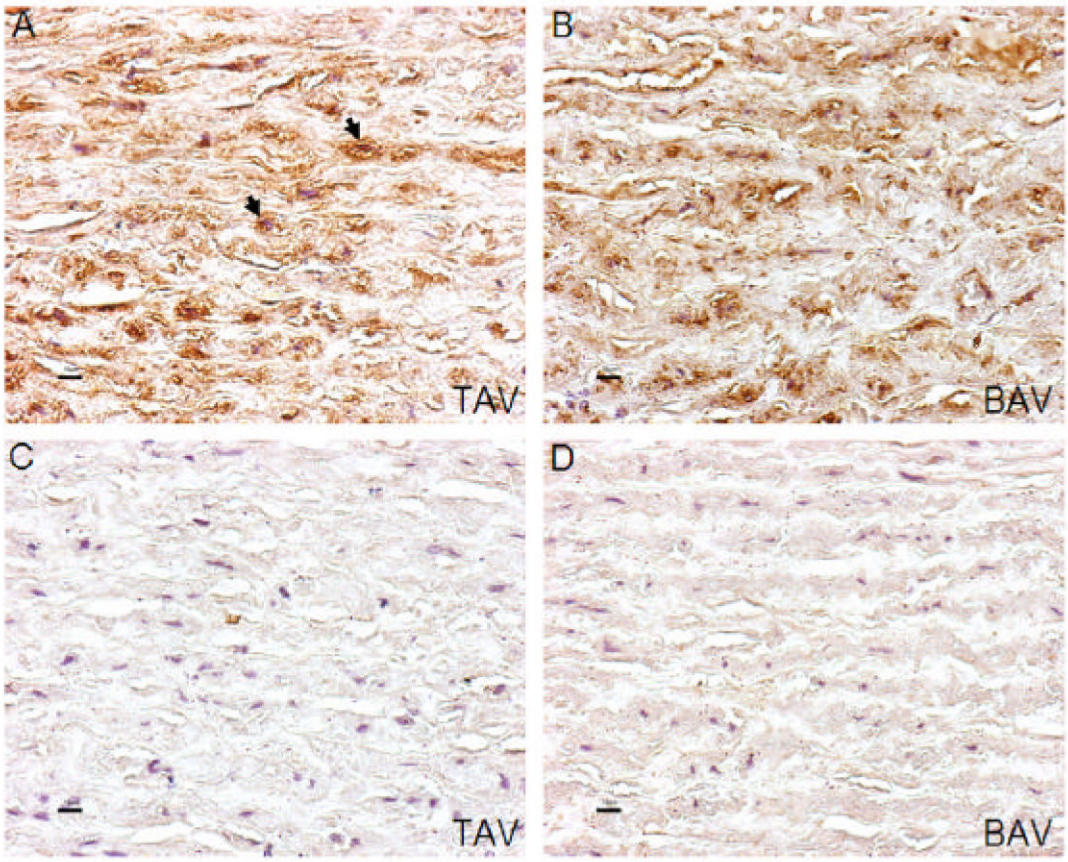

Figure 7.

Immunostaining of total HSP27 (with hematoxylin counterstain) in aortic samples of a patient with a TAV (A) and BAV (B), Figures C and D demonstrate the corresponding controls. Arrows in Figure A mark the accumulation of HSP27 staining inside the cytoplasma around the nuclei of VSMCs. Magnification in all images is x40.

TABLE 1

Patients' baseline characteristics

	2DE			ELISA		
Variables	**BAV** ***n=5***	**TAV** ***n=5***	**p-value**	**BAV** ***n=6***	**TAV** ***n=9***	**p-value**
Age*	49.2 ± 10.2	63.2 ± 8.6	0.1	48.5 ± 9.3	57.7 ± 7.9	0.1
Gender (female:male)	0:5	0:5	1	0:6	3:6	0.1
Max. aortic diameter (mm)*	59 ± 3.5	59.4 ± 2.8	0.8	58.3 ± 3.6	56.2 ± 4.4	0.4
Aortic valve insufficiency	1 (20%)	3 (60%)	0.2	2 (33%)	5 (56%)	0.4
Arterial Hypertension	1 (20%)	3 (60%)	0.2	3 (50%)	3 (33%)	0.5
Diabetes mellitus	0	0	-	0	0	-
Non-stenotic coronary artery disease	2 (40%)	2 (40%)	1	2 (33%)	2 (22%)	0.6
Dyslipidemia	0	2 (40%)	0.1	2 (33%)	3 (33%)	1
Smoking history	1 (20%)	3 (60%)	0.2	1 (17%)	3 (33%)	0.5
Preoperative dyspnea (=NYHA II)	2 (40%)	3 (60%)	0.5	2 (33%)	6 (67%)	0.2
LVEF (%)*	64.8 ± 4.8	56.8 ± 12.3	0.3	63.2 ± 5.8	58.5 ± 11.3	0.3
Preoperative medication						
Betablocker	2 (40%)	1 (20%)	0.5	2 (33%)	3 (33%)	1
ACE inhibitor/AT II antagonist	1 (20%)	3 (60%)	0.2	2 (33%)	6 (67%)	0.2
Aortic valve replacement	4 (80%)	4 (80%)	1	5 (83%)	6 (67%)	0.5
Ascending aorta replacement	3 (60%)	2 (40%)	0.5	4 (67%)	6 (67%)	1

Abbreviations: BAV=Bicuspid Aortic Valve; TAV=Tricuspid Aortic Valve; NYHA=New York Heart Association Classification,

* in mean ± SD

TABLE 2

List of phosphoproteins identified using MALDI-TOF mass spectrometer

Spot	Protein Identity	Accession No.*	Mass	Score	Protein function
1	Rho GDP dissociation inhibitor 1	gi76780069	23250	68	Regulates the GDP/GTP exchange reaction of Rho proteins, regulates actin cytoskeleton organisation.
2–5	Heat shock protein 27	gi662841	22427	105–107	Involved in stress resistance, regulates actin organization, supports the formation of actin stress fibres, stabilizes the integrity of the cell.
7	Myosin regulatory light chain 2	gi15809016	19696	80	Regulates cell contraction, but also organization of the actin cytoskeleton.
9	Calponin 3	gi19263471	36391	680	Part of the actin cytoskeleton, less involved in the contraction process.
11	Alkaline phosphatase precursor	gi2507183	57406	65	Enzyme used for the dephosphorylation experiment.

* Mascot search results from the NCBInr protein database.